J. Math. Computer Sci., 35 (2024), 169–181

Online: ISSN 2008-949X

Journal of Mathematics and Computer Science

Journal Homepage: www.isr-publications.com/jmcs

How does media coverage affect a COVID-19 pandemic model with direct and indirect transmission?

Ashraf Adnan Thirthar[a,*], Shireen Jawad[b], Kamal Shah[c], Thabet Abdeljawad[c]

[a]Department of Studies and Planning, University of Fallujah, Anbar, Iraq.

[b]Department of Mathematics, College of Science, University of Baghdad, Baghdad, Iraq.

[c]Department of Mathematics and Sciences, Prince Sultan University, P.O. Box 66833, 11586 Riyadh, Saudi Arabia.

Abstract

In this paper, a compartmental differential epidemic model of COVID-19 pandemic transmission is constructed and analyzed that accounts for the effects of media coverage. The model can be categorized into eight distinct divisions: susceptible individuals, exposed individuals, quarantine class, infected individuals, isolated class, infectious material in the environment, media coverage, and recovered individuals. The qualitative analysis of the model indicates that the disease-free equilibrium point is asymptotically stable when the basic reproduction number R_0 is less than one. Conversely, the endemic equilibrium is globally asymptotically stable when R_0 is bigger than one. In addition, a sensitivity analysis is conducted to determine which model parameters impact the fundamental reproduction number most. Finally, some numerical simulations are implemented to reinforce the theoretical part. The results of this study indicate that media coverage may serve as a viable strategy to impede the transmission of Covid-19.

Keywords: Covid-19, dynamical systems, stability, numerical simulation.

2020 MSC: 37Dxx, 34Dxx, 76Fxx.

1. Introduction

Mathematical modeling is the process of explaining systems, functions, and occurrences using mathematical ideas. Mathematical modeling has applications in almost every business, but it is most frequently employed in the fields of engineering, computer science, social science, and natural science. Based on your professional background and duties, you may need to apply this method to solve issues, provide explanations for events, and forecast outcomes. The core of many biological and ecological processes is the dynamic connections between species and their complex features [2, 5, 15–17, 22, 23, 25, 28, 30, 32]. The COVID-19 pandemic has disrupted our daily routine globally. People are now being afraid to do their natural activities publicly. COVID-19 is a shortened term for Severe Acute Respiratory Syndrome Coronavirus (SARS-CoV-2), a virus not previously known to exist in humans [20]. The virus was initially detected in Wuhan, a city in the Hubei region of China [33]. Subsequently, it quickly spread to more than

*Corresponding author

Email addresses: a.a.thirthar@uofallujah.edu.iq (Ashraf Adnan Thirthar), shireen.jawad@sc.uobaghdad.edu.iq (Shireen Jawad), kshah@psu.edu.sa; kamalshah408@gmail.com (Kamal Shah), tabdeljawad@psu.edu.sa (Thabet Abdeljawad)

doi: 10.22436/jmcs.035.02.04

Received: 2023-12-13 *Revised:* 2024-03-15 *Accepted:* 2024-03-30

200 countries. It was first identified in Wuhan City Hubei province of China [11], after that rapidly it has spread out over 200 countries. The pandemic has swallowed almost 0.82 million people's lives and infected more than 24.3 million people, as of August 24, 2020 [37]. In the last two decades, mankind already has faced two coronaviruses SARS [21] and MERS [8] but this time this pandemic has become more severe. Evidence has established that the virus is transmitted to people through respiratory droplets expelled by an infected individual during coughing, sneezing, or exhaling. However, evidence suggests that transmission can also occur through fomites near the sick individual. When a person infected with the virus breathes through the nose and throat, coughing or touching surfaces such as tables, doorknobs, and handrails can leave infected stems on objects and surfaces (known as fomite). Other people can become infected by touching these things or surfaces by touching their eyes, nose, or mouth before cleaning their hands. Guo et al. [14] conducted a study where they analyzed surface and air samples collected from an intensive care unit (ICU). During their investigation at Huoshenshan Hospital in Wuhan, China, researchers observed that the level of contamination was higher in the Intensive Care Unit (ICU) compared to the normal wards. They also discovered the virus was widely present on surfaces such as flooring, computer mice, trash cans, and sickbed handrails. Therefore, it can be inferred that the disease is transmitted directly and indirectly. The typical symptoms of COVID-19 include fever, weariness, dry cough, and myalgia. In addition, some individuals may experience headaches, abdominal pain, diarrhea, nausea, and vomiting. According to the authors, the projected fatality rate of this virus is approximately 4.5%. However, for the age group 70-79, it has increased to 8%. This condition poses a greater risk for elderly individuals who have comorbidities such as diabetes, asthma, and cardiovascular disease [9]. Elderly individuals with co-occurring conditions such as diabetes, asthma, or cardiovascular disease are especially vulnerable to this illness [24, 27].

Since the outbreak of this disease is ongoing and to date, no proper vaccine or medicine has been found in the market to cure COVID-19 thus a wave of fear has been created in the society. People are getting more and more scared when they see different kinds of news about this epidemic through the media. The media exerts a substantial impact on disseminating valuable information through different channels, such as community radio, television, print media, and the internet (e.g., journals and newspapers), thereby influencing the behavior of a community [10]. Consequently, it has a direct influence on the advancement of a pandemic [12, 13, 19, 29, 36]. As mathematical modeling is one of the finest ways to predict the dynamics of infectious diseases thus a lot of work has been done considering direct transmission of the pandemic COVID-19 [18], but there is little work considering direct as well as indirect transmission [1]. But there is no such work of COVID-19 by considering media effect with direct transmission as well as indirect transmission. Thus in this study, we mainly focused on these three important parts and developed a mathematical model for the COVID-19 outbreak. Numerous studies have demonstrated that when an epidemic strikes, people's behavior is altered by fear, which can lower the number of new cases. Thirthar et al. [31] take into consideration a SIS-B compartmental model with fear and treatment effects, taking into account the fact that an infected person can spread the disease to a susceptible individual.

We present a mathematical model that examines the dynamics of COVID-19 transmission, taking into account the impact of quarantine measures and media influence. The model starts by showing the total population size as N. This number is then split into eight separate groups: susceptible individuals $S(t)$, exposed individuals $E(t)$, quarantined individuals $Q(t)$, infected individuals $I(t)$, isolated individuals $J(t)$, infectious material in the environment $\nu(t)$, media coverage $M(t)$, and recovered individuals $R(t)$. So $N = S + E + Q + I + J + M + R$. The term "exposed class" refers to individuals who carry a low-level virus but are not thought to be infectious. In the quarantined category mandatory quarantine is mandated by the government to limit the likelihood of infection transmission. In the isolated class in which the patient is currently undergoing treatment in the hospital, infectious material represents material contaminated with infectious viruses. So this study incorporates a quarantine strategy and media effects and considers the transmission of the pandemic through both direct human-to-human contact and environmental sources contaminated with infectious viruses (indirect transmission), see Figure 1.

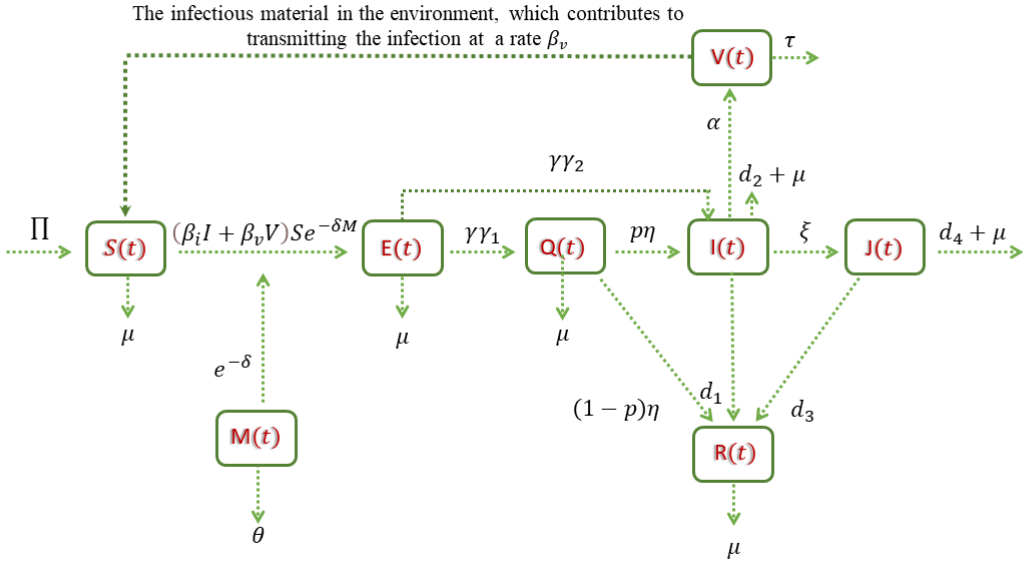

Figure 1: Flowchart of model (2.1).

The structure of the paper is as follows. A mathematical model has been formulated in Section 2. The fundamental characteristics of the system, such as positivity and boundedness, are detailed in Section 3. Section 4 provides a detailed discussion of several types of equilibria and their stability examination. In Section 5, we conduct numerical simulations to verify our conclusions. In Section 6, we provide a concise commentary.

2. Model formulation

Here, we have formulated a compartmental differential equation model with media effect for the COVID-19 pandemic. Depending on the status of the disease, the whole human population is separated into six sub-populations: susceptible class $S(t)$, exposed class $E(t)$ which consists of infected individuals not contagious to the community, exposed individuals quarantined at a rate of γ and designated as class $Q(t)$, symptomatic class (generated after the onset of clinical symptoms and included in infected class $I(t)$), isolated class $J(t)$ which consists of infected individuals who have developed clinical symptoms and have been isolated, and recovered class $R(t)$. According to some evidence, [26], the disease is transmitted not only through direct man to man but also through fomites in the immediate environment around the infected person. Thus in our model, we assume $V(t)$ represents the per capita infectious material in the environment and $M(t)$ represents the number of messages that all of them provide about the epidemic at time t. The total number of population at time t is given by $N(t) = S(t) + E(t) + Q(t) + I(t) + J(t) + R(t)$,

$$\begin{aligned}
\frac{dS}{dt} &= \Pi - (\beta_i I + \beta_v V)Se^{-\delta M} - \mu S, & \frac{dE}{dt} &= (\beta_i I + \beta_v V)Se^{-\delta M} - (\gamma + \mu)E,\\
\frac{dQ}{dt} &= \gamma_1\gamma E - (\eta + \mu)Q, & \frac{dI}{dt} &= \gamma_2\gamma E + p\eta Q - (\xi + d_1 + d_2 + \mu)I,\\
\frac{dJ}{dt} &= \xi I - (d_3 + d_4 + \mu)J, & \frac{dV}{dt} &= \alpha I - \tau V, \qquad (2.1)\\
\frac{dM}{dt} &= rM - \theta M, & \frac{dR}{dt} &= (1-p)\eta Q + d_1 I + d_3 J - \mu R.
\end{aligned}$$

As the seventh equation depends only on the M variable, we can discuss the following model

$$\begin{aligned}
\frac{dS}{dt} &= \Pi - (\beta_i I + \beta_v V)Se^{-\delta M} - \mu S, & \frac{dE}{dt} &= (\beta_i I + \beta_v V)Se^{-\delta M} - (\gamma + \mu)E,\\
\frac{dQ}{dt} &= \gamma_1\gamma E - (\eta + \mu)Q, & \frac{dI}{dt} &= \gamma_2\gamma E + p\eta Q - (\xi + d_1 + d_2 + \mu)I,\\
\frac{dJ}{dt} &= \xi I - (d_3 + d_4 + \mu)J, & \frac{dV}{dt} &= \alpha I - \tau V,\\
\frac{dR}{dt} &= (1-p)\eta Q + d_1 I + d_3 J - \mu R,
\end{aligned} \tag{2.2}$$

with initial conditions $S(0) > 0, E(0) \geqslant 0, Q(0) \geqslant 0, I(0) > 0, J(0) > 0, V(0) \geqslant 0, R(0) \geqslant 0$ and all the model parameters and their description are given in the following Table 1.

Table 1: Parameters and their descriptions.

Parameter	Description
Π	recruitment rate
β_i	rate of transmission for direct disease
β_v	rate of transmission for indirect disease
δ	rate at which disease-related message can influence the transmission rate
μ	natural death rate
γ	exposed people are quarantine rate
γ_1	The rate of people transferred from E to quarantine class
γ_2	The rate of people transferred from E to infected class
η	the rate at which quarantine people are infected
ξ	rate at which infected people are isolated
d_1	infected people recovery rate
d_2	disease-induced death rate
d_3	isolated people recovery rate
α	per capita rate of infectious material in the environment
τ	the mass-specific rate of loss of infectious material from the environment
$\mu_i,\ i = 1-6$	rate at which people may send the message about the epidemic
θ	the rate that message becomes outdated.
p	is the portion of symptomatic cases subject to infected
d_4	disease-induced death rate for isolated class

3. Basic properties

From a biological point of view, it is required to demonstrate that for any $t > 0$, all system solutions (2.2) with positive initial values will remain positive. Note that

$$\frac{dN}{dt} \leqslant \Pi - \mu N,$$

where $N(t) = S(t) + E(t) + Q(t) + I(t) + J(t) + R(t)$. As $t \to \infty$, the population $N(t)$ goes to $\frac{\Pi}{\mu}$, so the feasible region of human sub-model is

$$\Omega_N = \left\{(S, E, Q, I, J, R) \in R_+^6 : N \leqslant \frac{\Pi}{\mu}\right\}.$$

From pathogen population V, we get $\frac{dV}{dt} \leqslant \frac{\alpha\Pi}{\mu} - \tau V$ and $V(t) \leqslant \frac{\alpha\Pi}{\mu\tau}$, so the feasible region of pathogen sub-model is

$$\Omega_v = \left\{ V | 0 \leqslant V \leqslant \frac{\alpha\pi}{\mu\tau} \right\}.$$

It is easy to establish that the region $\Omega = \Omega_N \times \Omega_v$ is invariant. To prove this set is positive, from the first equation of (2.2) we obtain

$$\frac{dS}{dt} \geqslant -(\beta_i I + \beta_v V) S e^{-\delta M} - \mu S.$$

By using Ω_N and Ω_v,

$$\frac{dS}{dt} \geqslant -\left(\beta_i \frac{\pi}{\mu} + \beta_v \frac{\alpha\pi}{\mu\tau} - \mu \right) S.$$

Integrating both sides by separation of variables gives

$$S(t) \geqslant S(0) e^{-\int \left(\beta_i \frac{\pi}{\mu} + \beta_v \frac{\alpha\pi}{\mu\tau} - \mu \right) dt}.$$

Similarly, we can prove the positiveness of all equations of system (2.2).

4. Equilibria and their stability

System (2.2) has the following equilibrium points.

- Unique disease-free equilibrium point $D_0 = (\frac{\Pi}{\mu}, 0, 0, 0, 0, 0, 0)$.
- Endemic equilibrium point $D^* = (S^*, E^*, Q^*, I^*, J^*, V^*, R^*)$, where

$$\begin{cases} S^* = \frac{\pi}{\left(\beta_i I + \frac{\alpha}{\tau}\beta_v I^* - \mu\right) e^{-\delta M}}, \\ E^* = \frac{\pi(\beta_i + \frac{alpha}{\tau}\beta_v) I^*}{(\gamma+\mu)(\beta_i I^* + \frac{\alpha}{\tau}\beta v I^* - \mu)}, \\ Q^* = \frac{\gamma_1 \gamma}{\eta+\mu} E^*, \\ J^* = \frac{\zeta}{d_3+d_4+\mu} I^*, \\ V^* = \frac{alpha}{\tau} I^*, \\ R^* = \frac{1}{\mu}\left[d_1 + d_3 \frac{\zeta}{d_3+d_4+\mu} + (1-p)\eta \frac{(\gamma_1\gamma)}{(\eta+\mu)} \frac{\pi(\beta_i + \frac{\alpha}{\tau}\beta_v}{(\gamma+\mu)(\beta_i I^* + \frac{\alpha}{\tau}\beta_v I^* - \mu)} \right] I^*, \\ I^* = \frac{[\gamma_2\gamma(\eta+\mu) + \gamma\gamma_1 p\eta][\pi(\beta_i + \frac{\alpha}{\tau}\beta_v)] - \mu(\zeta + d_1 + d_2 + \mu)}{(\eta+\mu)(\gamma+\mu)(\beta_i + \frac{\alpha}{\tau}\beta_v)(\zeta + d_1 + d_2 + \mu)}. \end{cases}$$

Using next generation matrix method the basic reproduction number is given by

$$R_0 = \frac{\Pi(\beta_i + \beta_v \alpha)(p\eta\gamma\gamma_1 + \eta\gamma\gamma_2 + \mu\gamma\gamma_2)}{\mu(\xi + d_1 + d_2 + \mu)(\gamma + \mu)(\eta + \mu)}.$$

Here in Figure 2, we present 3D profile of R_0 against various values of parameters involved in its calculation.

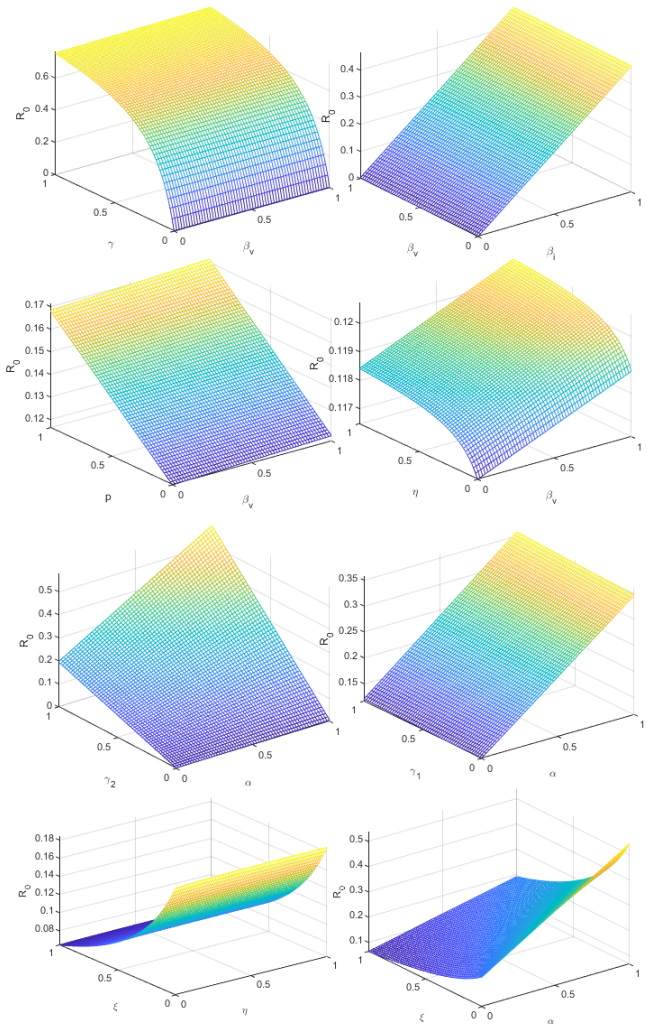

Figure 2: 3D profile of R_0.

4.1. *Sensitivity of* R_0

Here, we present sensitivity of R_0 in figure 3 as follows. Here to discuss the sensitivity analysis of R_0,

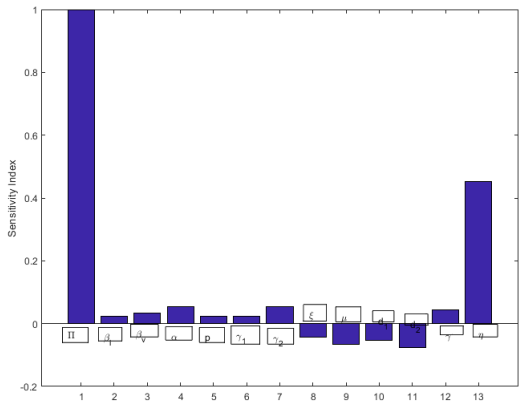

Figure 3: Sensitivity index presentation used in the R_0 computation.

we use the famous role described by $\mathbf{S}_q^{R_0} = \frac{q}{R_0}\frac{\partial R_0}{\partial q}$,

$$\mathbf{S}_{\Pi}^{R_0} = \frac{\Pi}{R_0}\frac{\partial R_0}{\partial \Pi} = 1 > 0, \quad \mathbf{S}_{\beta_i}^{R_0} = \frac{\beta_i}{R_0}\frac{\partial R_0}{\partial \beta_i} = 0.0234 > 0, \quad \mathbf{S}_{\beta_v}^{R_0} = \frac{\beta_v}{R_0}\frac{\partial R_0}{\partial \beta_v} = 0.03456 > 0,$$
$$\mathbf{S}_{\alpha}^{R_0} = \frac{\alpha}{R_0}\frac{\partial R_0}{\partial \alpha} = 0.05432, \quad \mathbf{S}_{p}^{R_0} = \frac{p}{R_0}\frac{\partial R_0}{\partial p} = 0.04532, \quad \mathbf{S}_{\gamma_1}^{R_0} = \frac{\gamma_1}{R_0}\frac{\partial R_0}{\partial \gamma_1} = 0.02234,$$
$$\mathbf{S}_{\gamma_2}^{R_0} = \frac{\gamma_2}{R_0}\frac{\partial R_0}{\partial \gamma_2} = 0.02356, \quad \mathbf{S}_{\gamma}^{R_0} = \frac{\gamma}{R_0}\frac{\partial R_0}{\partial \gamma} = 0.05432, \quad \mathbf{S}_{\mu}^{R_0} = \frac{\mu}{R_0}\frac{\partial R_0}{\partial \mu} = -0.04321,$$
$$\mathbf{S}_{\xi}^{R_0} = \frac{\xi}{R_0}\frac{\partial R_0}{\partial \xi} = -0.065432, \quad \mathbf{S}_{d_1}^{R_0} = \frac{d_1}{R_0}\frac{\partial R_0}{\partial d_1} = -0.05431, \quad \mathbf{S}_{d_2}^{R_0} = \frac{d_2}{R_0}\frac{\partial R_0}{\partial d_2} = -0.07652,$$
$$\mathbf{S}_{\eta}^{R_0} = \frac{p}{R_0}\frac{\partial R_0}{\partial \eta} = 0.4321 > 0.$$

Theorem 4.1. *The disease-free equilibrium point* D_0 *is locally asymptotically stable if* $R_0 < 1$ *and unstable if* $R_0 > 1$.

Proof. The Jacobian matrix of system (2.2) in general is $J = [C_{ij}], i, j = 0, 1, 2, \ldots, 7$, where $C_{11} = -(\beta_i I + \beta_v V)e^{-\delta M} - \mu$, $C_{14} = -\beta_i S e^{-\delta M}$, $C_{21} = (\beta_i I + \beta_v V)e^{-\delta M}$, $C_{24} = \beta_i S e^{-\delta M}$, $C_{32} = \gamma\gamma_1$, $C_{33} = -(\gamma + \mu)$, $C_{42} = \gamma\gamma_2$, $C_{43} = p\eta$, $C_{44} = -(\xi + d_1 + d_2 + \mu)$, $C_{54} = \xi$, $C_{55} = -(d_3 + d_4 + \mu)$, $C_{64} = \alpha$, $C_{66} = -\tau$, $C_{73} = (1-p)\eta$, $C_{74} = d_1$, $C_{75} = d_3$, $C_{77} = -\mu$ and all other entries are zero. So, the characteristic equation of Jacobian matrix of (2.2) around D^* is given by

$$(C_{77} - \lambda)(C_{55} - \lambda)(C_{66} - \lambda)(\lambda^4 + A\lambda^3 + B\lambda^2 + C\lambda + D) = 0,$$

where $A = -(C_{11} + C_{33} + C_{44}) = -(C_{11} + \Upsilon_1)$, $B = C_{33}C_{44} + C_{24}C_{42} = \Upsilon_2 + \Upsilon_3$, $C = C_{11}C_{33} + C_{11}C_{44} - C_{11}C_{33}C_{44} + C_{24}C_{33}C_{42} + C_{24}C_{32}C_{43} - C_{11}C_{24}C_{42} - C_{42} = \Upsilon_4 + \Upsilon_5$, $D = (C_{32}C_{43} - C_{33}C_{42})(C_{11}C_{24} - C_{21}C_{14}) = \Upsilon_6\Upsilon_7$, where $\Upsilon_1 = C_{33} + C_{44}$, $\Upsilon_2 = C_{33}C_{44}$, $\Upsilon_3 = C_{24}C_{42}$, $\Upsilon_4 = C_{11}C_{33} + C_{11}C_{44} - C_{11}C_{33}C_{44} + C_{24}C_{32}C_{43} - C_{11}C_{24}C_{42}$, $\Upsilon_5 = C_{24}C_{33}C_{42} - C_{42}$, $\Upsilon_6 = C_{32}C_{43} - C_{33}C_{42}$, $\Upsilon_7 = C_{11}C_{24} - C_{21}C_{14}$. It is easy to show that $\Upsilon_2, \Upsilon_3, \Upsilon_4$, and Υ_6 are positive terms and $C_{77}, C_{55}, C_{44}, \Upsilon_1, \Upsilon_5, \Upsilon_7, A$, and B are negative terms, and the conditions $\Upsilon_4 > \Upsilon_5 I^*(\xi + d_1 + d_2 + \mu) \geqslant S^*\gamma\gamma_2$ and $\gamma\gamma_2 \geqslant \beta_i S^* e^{-\delta M^*}$ are sufficient conditions to make C and D positive. By a straightforward computation, we can verify that

$$ABC - C^2 - A^2D = -(C_{11} + \Upsilon_1) + (\Upsilon_2 + \Upsilon_3)(\Upsilon_4 + \Upsilon_5) - (\Upsilon_4 + \Upsilon_5)^2 - (C_{11} + \Upsilon_1)^2\Upsilon_6\Upsilon_7.$$

This is positive provided to

$$\Upsilon_6\Upsilon_7(C_{11}^2 + \Upsilon_1^2) > \Upsilon_4^2 + \Upsilon_5^2,$$

which ensures the local stability of the endemic equilibrium point D^*. □

Theorem 4.2. *The disease-free equilibrium point* D_0 *is globally asymptotically stable if* $R_0 < 1$ *and unstable if* $R_0 > 1$.

Proof. We can rewrite the system (2.2) as

$$\frac{dX}{dt} = F(X, W), \quad \frac{dW}{dt} = H(X, W), \quad H(X, 0) = 0,$$

where $X = (S, R)$ is the number of uninfected individuals compartments and $W = (E, Q, I, J, V)$ is the number of infected individuals. Now if the following two conditions are satisfied then it ensures the global stability of the disease-free equilibrium point D_0:

(i) for $\frac{dX}{dt} = F(X, 0)$, X^* is globally stable; and
(ii) $H(X, W) = BW - \hat{H}(X, W)$, $\hat{H}(X, W) \geqslant 0$ for $(X, W) \in \Omega_v$,

where, $B = D_V H(X^*, 0)$ denotes the Metzler matrix and Ω_v is the positively invariant set. Now we use the formula of Castillo-Cavez [7], and we get for our system:

$$F(X,0) = \begin{bmatrix} \pi - \mu S \\ 0 \end{bmatrix},$$

$$B = \begin{bmatrix} -(\gamma+\mu) & 0 & \beta_i S & 0 & \beta_v S \\ \gamma\gamma_1 & -(\eta+\mu) & 0 & 0 & 0 \\ \gamma\gamma_2 & p\eta & -(\xi + d_1 + d_2 + \mu) & 0 & 0 \\ 0 & 0 & \xi & -(d_3+d_4+\mu) & 0 \\ 0 & 0 & \alpha & 0 & -\tau \end{bmatrix},$$

$$\hat{H}(X,W) = \begin{bmatrix} (\beta_i + \beta_v) S(1 - e^{-\delta M}) \\ 0 \\ 0 \\ 0 \end{bmatrix}.$$

Clearly, it can be shown that $\hat{H}(X,W) \geqslant 0$ when the state variables are inside Ω_v. Also $X^* = (\frac{\pi}{\mu}, 0)$ is globally stable equilibrium of the system $\frac{dX}{dt} = F(X,0)$. Hence the theorem follows. □

Next, we used the direct Lyapunov approach to study global stability. By demonstrating that the derivative of the Lyapunov function is less than or equal to one, we were able to show that these points are globally asymptotically stable.

Theorem 4.3. *The endemic equilibrium point* D^* *is globally asymptotically stable if* $R_0 < 1$.

Proof. Consider a suitable Lyapunov function

$$V(S,E,Q,I,J,V,R) = \frac{1}{2}(S-S^*)^2 + \frac{1}{2}(E-E^*)^2 + \frac{1}{2}(Q-Q^*)^2 + \frac{1}{2}(I-I^*)^2 + \frac{1}{2}(J-J^*)^2 + \frac{1}{2}(V-V^*)^2 + \frac{1}{2}(R-R^*)^2.$$

Now differentiating $V(S,E,Q,I,J,V,R)$ with respect to the solution of system (2.2) we obtain

$$\begin{aligned} \frac{dV}{dt} &= (S-S^*)\dot{S} + (E-E^*)\dot{E} + (Q-Q^*)\dot{Q} + (I-I^*)\dot{I} + (J-J^*)\dot{J} + (V-V^*)\dot{V} + (R-R^*)\dot{R} \\ &= (S-S^*)\Big\{\pi - (\beta_i I + \beta_v V)Se^{-\delta M} - \mu S\Big\} + (E-E^*)\Big\{(\beta_i I + \beta_v V)Se^{-\delta M} - (\gamma+\mu)E\Big\} \\ &\quad + (Q-Q^*)\Big\{\gamma\gamma_1 E - (\eta+\mu)Q\Big\} + (I-I^*)\Big\{\gamma\gamma_2 E + p\eta Q - (\xi + d_1 + d_2 + \mu)I\Big\} \\ &\quad + (J-J^*)\Big\{\xi I - (d_3+d_4+\mu)J\Big\} + (V-V^*)\Big\{\alpha I - \tau V\Big\} + (R-R^*)\Big\{(1-p)\eta Q + d_1 I + d_3 J - \mu R\Big\}. \end{aligned}$$

Assume $f(M) = e^{-\delta M}$, then $f'(M) = -\delta e^{-\delta M}$. Now, applying Lagrange MVT, we obtain $|f(M^*) - f(M)| = |f'(c)||M - M^*|$, where $M < c < M^*$. Therefore

$$\begin{aligned} \frac{dV}{dt} &\leqslant -|S-S^*|^2\Big\{\mu - f(M^*)(\beta_i I^* + \beta_v V^*)\Big\} - (\gamma+\mu)|E-E^*|^2 - (\eta+\mu)|Q-Q^*|^2 \\ &\quad - (\xi + d_1 + d_2 + \mu)|I-I^*|^2 - (d_3+d_4+\mu)|J-J^*|^2 - \tau|V-V^*|^2 - \mu|R-R^*|^2 \\ &\quad + \gamma\gamma_1|E-E^*||Q-Q^*| + (\gamma\gamma_2 + \frac{\pi}{\mu})|E-E^*||I-I^*| + p\eta|Q-Q^*||I-I^*| \\ &\quad + \xi|I-I^*||J-J^*| + \alpha|I-I^*||V-V^*| + (1-p)\eta|Q-Q^*||R-R^*| + d_1|I-I^*||R-R^*| \\ &\quad + d_3|J-J^*||R-R^*| + \beta_i\frac{\pi}{\mu}I^*|E-E^*||M-M^*| + \beta_i\frac{\pi}{\mu}I^*|S-S^*||M-M^*| \\ &\quad + I^* f(M^*)|S-S^*||E-E^*| + \frac{\pi}{\mu}|S-S^*||I-I^*| + \beta_v\frac{\pi}{\mu}V^*|E-E^*||M-M^*| + \beta_v\frac{\pi}{\mu}V^*|S-S^*||M-M^*| \\ &\quad + V^* f(M^*)|S-S^*||E-E^*| + \frac{\pi}{\mu}|S-S^*||V-V^*| + \frac{\pi}{\mu}|E-E^*||V-V^*| \leqslant -X^T P X, \end{aligned}$$

where

$$X = \begin{bmatrix} |S-S^*| \\ |E-E^*| \\ |Q-Q^*| \\ |I-I^*| \\ |J-J^*| \\ |V-V^*| \\ |R-R^*| \end{bmatrix}, \quad P = (a_{ij})_{7\times 7} = \begin{bmatrix} a_{11} & a_{12} & a_{13} & a_{14} & a_{15} & -\tau & -\mu \\ 0 & \gamma\gamma_1 & a_{23} & p\eta & \xi & \alpha & (1-p)\eta \\ 0 & 0 & 0 & d_1 & 0 & d_3 & a_{37} \\ a_{41} & 0 & 0 & 0 & 0 & 0 & 0 \\ I^*f(M^*) & a_{52} & 0 & 0 & 0 & 0 & 0 \\ \frac{\pi}{\mu} & V^*f(M^*) & 0 & 0 & 0 & \frac{\pi}{\mu} & 0 \\ a_{71} & 0 & 0 & 0 & 0 & \frac{\pi}{\mu} & 0 \end{bmatrix},$$

where $a_{11} = -\Big\{\mu - f(M^*)(\beta_i I^* + \beta_v V^*)\Big\}$, $a_{12} = -(\gamma+\mu)$, $a_{13} = -(\eta+\mu)$, $a_{14} = -(\xi + d_1 + d_2 + \mu)$, $a_{15} = -(d_3 + d_4 + \mu)$, $a_{23} = (\gamma\gamma_2 + \frac{\pi}{\mu})$, $a_{37} = \beta_i \frac{\pi}{\mu} I^*|M - M^*|$, $a_{41} = \beta_i \frac{\pi}{\mu} I^*|M - M^*|$, $a_{52} = \beta_v \frac{\pi}{\mu} V^*|M - M^*|$, and $a_{71} = \beta_v \frac{\pi}{\mu} V^*|M - M^*|$. □

5. Numerical simulation

In this section, we will illustrate the theoretical part with some numerical simulations. To this end, we will take the proposed model (2.2) with different initial conditions. The system is solved numerically using six-order Runge-Kutta predictor-adjusted methods in order to investigate the global behavior of the solution of system (2.2) further. To choose the control set of parameters, the impact of changing the parameters on the solution is also examined. The majority of the results are displayed using Matlab as time series. The parameter values of the model (2.2) are chosen as $\pi = 1$, $\mu = 0.2$, $\beta_i = 0.253$, $\beta_v = 0.5$, $\delta = 0.04$, $\gamma = 0.03$, $\gamma_1 = 0.4$, $\gamma_2 = 0.6$, $d_1 = 0.2$, $d_2 = 0.15$, $d_3 = 0.01$, $d_4 = 0.4$, $\alpha = 0.005$, $\tau = 0.4$, $p = 0.03$, $\eta = 0.4$, $\xi = 0.3$, $r = 0.002$, and $\theta = 0.003$.

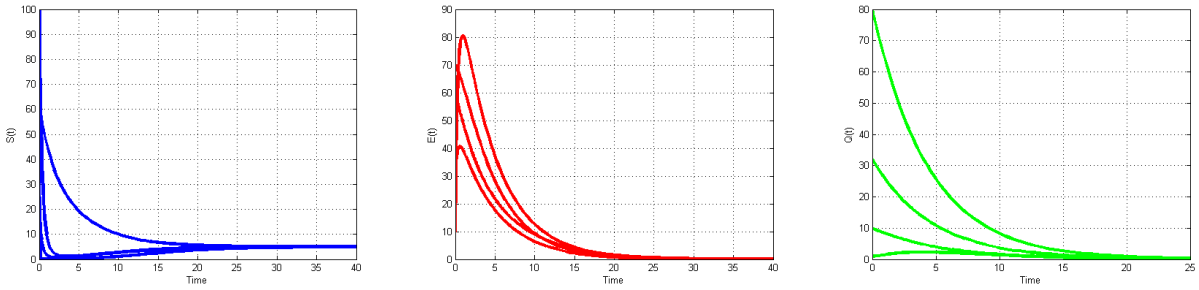

(a) S(t) (b) E(t) (c) Q(t)

Figure 4: The time series of $S(t)$, $E(t)$ and $Q(t)$ with the above parameters. In this case $R_0 = 0.1180 < 1$.

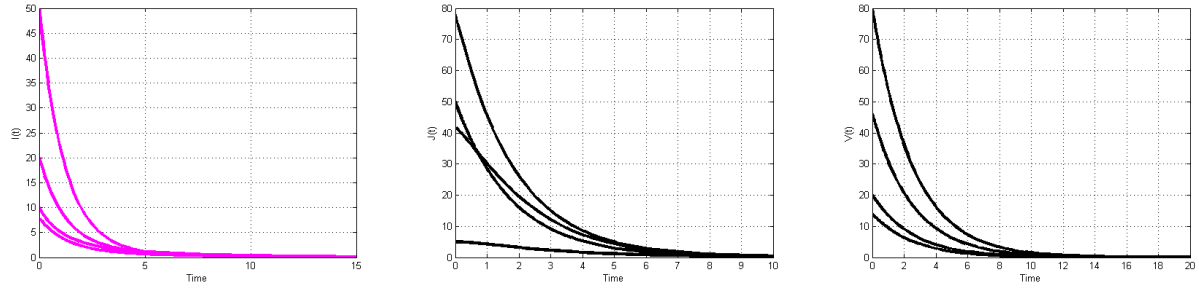

(a) I(t) (b) J(t) (c) V(t)

Figure 5: The time series of $I(t)$, $J(t)$, and $V(t)$ with the above parameters. In this case $R_0 = 0.1180 < 1$.

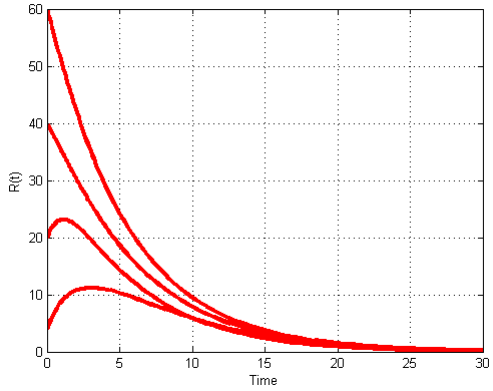

Figure 6: The time series of $R(t)$ with the above parameters. In this case $R_0 = 0.1180 < 1$.

In the Figures 4, 5, and 6, we have implemented the dynamics of the solution of our model (2.2) in the case of the basic reproduction number R_0 less than one. We observe that all the solutions converge to zero except that of $S(t)$ which converges to $\frac{\pi}{\mu}$ which is the disease-free equilibrium point. Biologically speaking, when we are in the case $R_0 = 0.1180 < 1$, the disease will die out from the population.

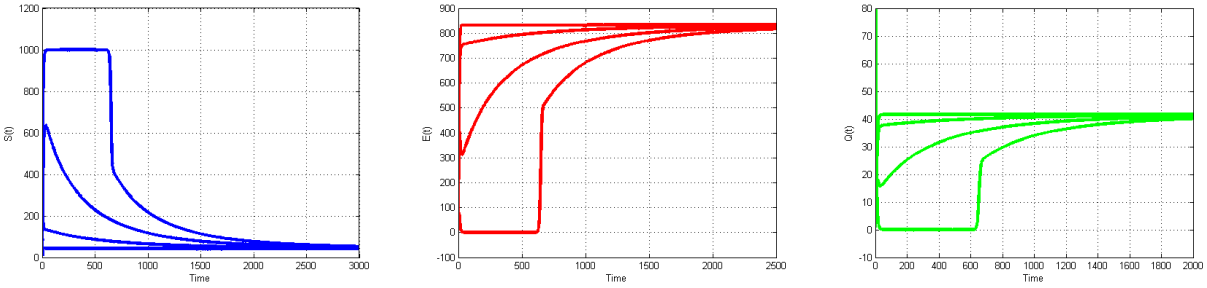

(a) S(t) (b) E(t) (c) Q(t)

Figure 7: The time series of $S(t)$, $E(t)$, and $Q(t)$ with the above parameters except $\pi = 200$. In this case $R_0 = 23.6027 > 1$.

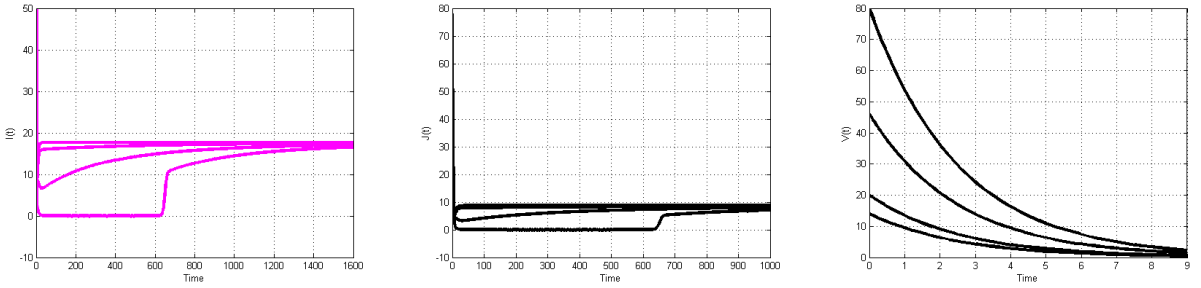

(a) I(t) (b) J(t) (c) V(t)

Figure 8: The time series of $I(t)$, $J(t)$, and $V(t)$ with the above parameters except $\pi = 200$. In this case $R_0 = 23.6027 > 1$.

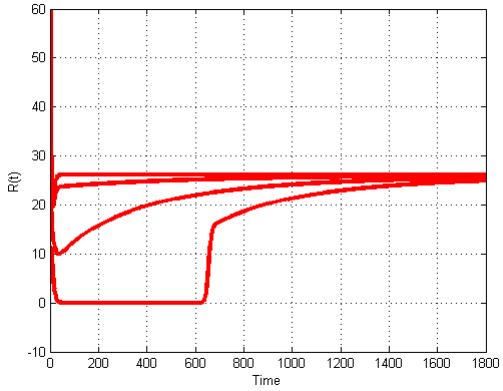

Figure 9: The time series of $R(t)$ with the above parameters except $\pi = 200$. In this case $R_0 = 23.6027 > 1$.

In the Figures 7, 8, and 9, we have plotted the evolutions of the solution when the basic reproduction number R_0 is greater than one. One can see that all the curves converge to the endemic equilibrium D^* at a certain time and keep these values forever. That means the endemic equilibrium is globally asymptotically stable.

For more illustration, let us draw the dynamic of R_0 with respect to some parameters of our model (2.2). From the Figures 10 and 11, we observe that the basic reproduction number R_0 is an increasing function with respect to the parameters β_i, μ, η, and ξ.

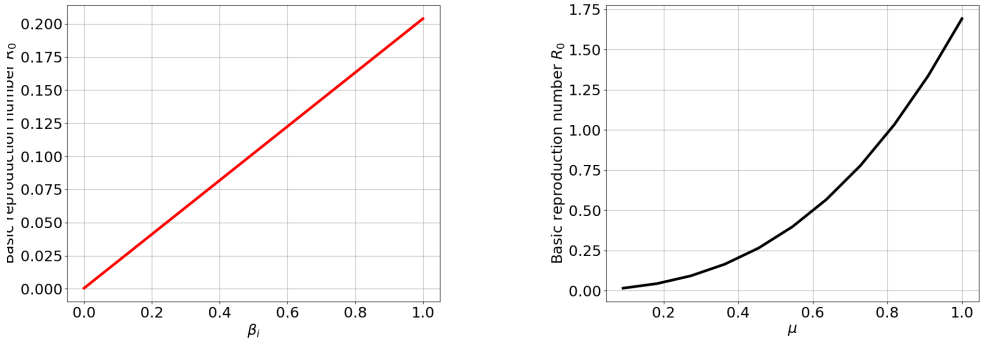

Figure 10: Dynamics of R_0 with respect to β_i and μ.

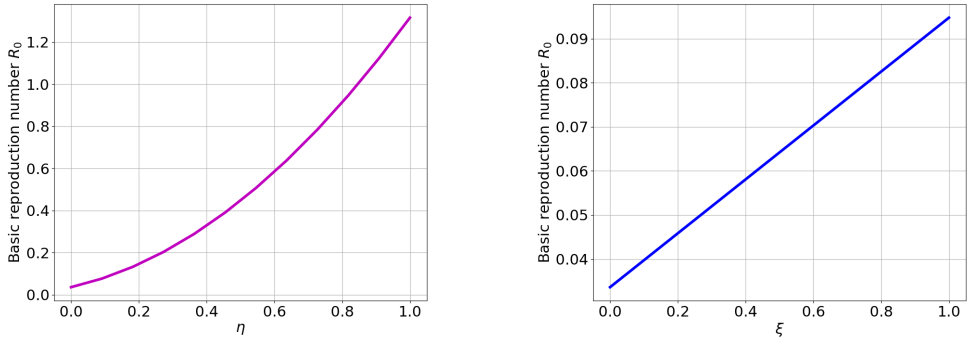

Figure 11: Dynamics of R_0 with respect to η and ξ.

Several important methods for finding the solutions to the governing equations have been described; however, certain recently developed methods, such as the fractional iteration algorithm, should also be added and discussed rather than just being named see [3, 4, 6].

6. Discussion

We have proposed and studied a deterministic epidemic model that describes the effects of media coverage on the transmission dynamics of COVID-19. It is shown that the considered model admits two equilibrium points. Moreover, we have proved that the disease-free equilibrium D_0 is globally asymptotically stable when $R_0 < 1$ and the endemic equilibrium D^* is globally asymptotically stable for $R_0 > 1$. For different initial conditions, we have plotted the curves of the solutions for both cases $R_0 < 1$ and $R_0 > 1$. In the last part of this work, we have implemented the evolution of the basic reproduction number R_0 with respect to some parameters of the model. We observe from the Figures 10 and 11 that we have to reduce the values of the parameters β_i, μ, η, and ξ to keep R_0 less than unity. Here are a few possible paths our research may take in the future.

- Considerations for space: Expand our model to include dynamics in space. Since geographical factors are frequently present in ecological systems, taking spatial factors into account can help us understand how populations and epidemics move more realistically.
- Interactions between multiple classes: Consider extending our model to include interactions with multiple classes. Epidemic systems are often characterized by complex interactions between multiple classes, and understanding these interactions can provide a more comprehensive view of the dynamics of the epidemiological system.
- Memory effect: It is possible to study state memory as a term of fractional orders of the current model [34, 35, 38].

Acknowledgment

The authors K.Shah and T. Abdeljawad would like to thank Prince Sultan University for paying the APC and support through the TAS research lab.

References

[1] M. S. Abdo, A. S. Alghonaim, B. A. Essam, *Public perception of COVID-19's global health crisis on Twitter until 14 weeks after the outbreak*, Digit. Scholarsh. Humanit., **36** (2021), 509–524. 1
[2] M. Ahmed, S. Jawad, *The role of antibiotics and probiotics supplements on the stability of gut flora bacteria interactions*, Commun. Math. Biol. Neurosci., **2023** (2023), 1–20. 1
[3] H. Ahmad, T. A. Khan, I. Ahmad, P. S. Stanimirović, Y.-M. Chu, *A new analyzing technique for nonlinear time fractional Cauchy reaction diffusion model equations*, Results Phys., **19** (2020). 5
[4] H. Ahmad, A. R. Seadawy, T. A. Khan, *Study on numerical solution of dispersive water wave phenomena by using a reliable modification of variational iteration algorithm*, Math. Comput. Simulation, **177** (2020), 13–23. 5
[5] M. Al Nuaimi, S. Jawad, *Persistence and bifurcation analysis among four species interactions with the influence of competition, predation and harvesting*, Iraqi J. Sci., **64** (2023), 1369–1390. 1
[6] O. Bazighifan, H. Ahmad, S.-W. Yao, *New oscillation criteria for advanced differential equations of fourth order*, Mathematics, **8** (2020), 1–10. 5
[7] C. Castillo-Chavez, *On the computation of R, and its role on global stability Carlos Castillo-Chavez, Zhilan Feng, and Wenzhang Huang*, Springer, New York, (2002). 4.1
[8] A. Chafekar, B. C. Fielding, *MERS-CoV: understanding the latest human coronavirus threat*, Viruses, **10** (2018), 1–22. 1
[9] R. Chen, W. Liang, M. Jiang, W. Guan, C. Zhan, T. Wang, C. Tang, L. Sang, J. Liu, Z. Ni, Y. Hu, L. Liu, H. Shan, C. Lei, Y. Peng, L. Wei, Y. Liu, Y. Hu, P. Peng, J. Wang, N. Zhong, *Risk factors of fatal outcome in hospitalized subjects with coronavirus disease 2019 from a nationwide analysis in China*, Chest, **158** (2020), 97–105. 1
[10] M. Cinelli, W. Quattrociocchi, A. Galeazzi, C. M. Valensise, E. Brugnoli, A. L. Schmidt, P. Zola, F. Zollo, A. Scala, *The COVID-19 social media infodemic*, Sci. Rep., **10** (2020), 1–10. 1

[11] D. Cucinotta, M. Vanelli, *WHO declares COVID-19 a pandemic*, Acta Biomed., **91** (2020), 157–160. 1
[12] A. Devi, A. Kumar, D. Baleanu, A. Khan, *On stability analysis and existence of positive solutions for a general non-linear fractional differential equations*, Adv. Difference Equ., **2020** (2020), 16 pages. 1
[13] A. Goel, L. Gupta, *Social media in the times of COVID-19*, J. Clin. Rheumatol., **26** (2020), 220–223. 1
[14] Z.-D. Guo, Z.-Y. Wang, S.-F. Zhang, X. Li, L. Li, C. Li, Y. Cui, R.-B. Fu, Y.-Z. Dong, X.-Y. Chi, M.-Y. Zhang, K. Liu, C. Cao, B. Liu, K. Zhang, Y.-W. Gao, B. Lu, W. Chen, *Aerosol and surface distribution of severe acute respiratory syndrome coronavirus 2 in hospital wards, Wuhan, China, 2020*, Emerg. Infect. Dis., **26** (2020), 1586–1591. 1
[15] S. K. Hassan, S. R. Jawad, *The Effect of Mutual Interaction and Harvesting on Food Chain Model*, Iraqi J. Sci., (2022), 2641–2649. 1
[16] S. Jawad, S. K. Hassan, *Bifurcation analysis of commensalism intraction and harvisting on food chain model*, Brazilian J. Biometrics, **41** (2023), 218–233.
[17] S. Jawad, M. Winter, Z.-A. S. A. Rahman, Y. I. A. Al-Yasir, A. Zeb, *Dynamical behavior of a cancer growth model with chemotherapy and boosting of the immune system*, Mathematics, **11** (2023), 1–16. 1
[18] H. Khan, F. Ahmad, O. Tunç, M. Idrees, *On fractal-fractional Covid-19 mathematical model*, Chaos Solitons Fractals, **157** (2022), 11 pages. 1
[19] H. Khan, J. F. Gómez-Aguilar, A. Alkhazzan, A. Khan, *A fractional order HIV-TB coinfection model with nonsingular Mittag-Leffler law*, Math. Methods Appl. Sci., **43** (2020), 3786–3806. 1
[20] F. Krammer, *SARS-CoV-2 vaccines in development*, Nature, **586** (2020), 516–527. 1
[21] Q.-X. Long, X.-J. Tang, Q.-L. Shi, Q. Li, H.-J. Deng, J. Yuan, J.-L. Hu, W. Xu, Y. Zhang, F.-J. Lv, K. Su, F. Zhang, J. Gong, B. Wu, X.-M. Liu, J.-J. Li, J.-F. Qiu, J. Chen, A.-L. Huang, *Clinical and immunological assessment of asymptomatic SARS-CoV-2 infections*, Nat. Med., **26** (2020), 1200–1204. 1
[22] I. Masti, K. Sayevand, H. Jafari, *On epidemiological transition model of the Ebola virus in fractional sense*, J. Appl. Anal. Comput., **14** (2024), 1625–1647. 1
[23] I. Masti, K. Sayevand, H. Jafari, *On analyzing two dimensional fractional order brain tumor model based on orthonormal Bernoulli polynomials and Newton's method*, Int. J. Optim. Control. Theor. Appl. IJOCTA, **14** (2024), 12–19. 1
[24] R. K. Naji, A. A. Thirthar, *Stability and bifurcation of an SIS epidemic model with saturated incidence rate and treatment function*, Iran. J. Math. Sci. Inform., **15** (2020), 129–146. 1
[25] K. Sayevand, V. Moradi, *A robust computational framework for analyzing fractional dynamical systems*, Discrete Contin. Dyn. Syst. Ser. S, **14** (2021), 3763–3783. 1
[26] A. G. M. Selvam, J. Alzabut, D. A. Vianny, M. Jacintha, F. B. Yousef, *Modeling and stability analysis of the spread of novel coronavirus disease COVID-19*, Int. J. Biomath., **14** (2021), 34 pages. 2
[27] Z. Shahid, R. Kalayanamitra, B. McClafferty, D. Kepko, D. Ramgobin, R. Patel, C. S. Aggarwal, R. R. Vunnam, N. Sahu, D. Bhatt, K. Jones, R. Golamari, R. Jain, *COVID-19 and older adults: what we know*, J. Am. Geriatr. Soc., **68** (2020), 926–929. 1
[28] R. N. Shalan, R. Shireen, A. H. Lafta, *Discrete an SIS model with immigrants and treatment*, J. Interdiscip. Math., **24** (2021), 1201–1206. 1
[29] H. Tajadodi, A. Khan, J. F. Gómez-Aguilar, H. Khan, *Optimal control problems with Atangana-Baleanu fractional derivative*, Optimal Control Appl. Methods, **42** (2021), 96–109. 1
[30] A. A. Thirthar, *A mathematical modelling of a plant-herbivore community with additional effects of food on the environment*, Iraqi J. Sci., **64** (2023), 3551–3566. 1
[31] A. A. Thirthar, H. Abboubakar, A. Khan, T. Abdeljawad, *Mathematical modeling of the COVID-19 epidemic with fear impact*, AIMS Math., **8** (2023), 6447–6465. 1
[32] A. A. Thirthar, S. J. Majeed, K. Shah, T. Abdeljawad, *The dynamics of an aquatic ecological model with aggregation, Fear and Harvesting Effects*,, AIMS Math., **7** (2022), 18532–18552. 1
[33] A. A. Thirthar, R. K. Naji, F. Bozkurt, A. Yousef, *Modeling and analysis of an SI1I2R epidemic model with nonlinear incidence and general recovery functions of I1*, Chaos Solitons Fractals, **145** (2021), 1–9. 1
[34] A. A. Thirthar, P. Panja, A. Khan, M. A. Alqudah, T. Abdeljawad, *An ecosystem model with memory effect considering global warming phenomena and an exponential fear function*, Fractals, **31** (2023), 1–29. 6
[35] A. A. Thirthar, N. Sk, B. Mondal, M. A. Alqudah, T. Abdeljawad, *Utilizing memory effects to enhance resilience in disease-driven prey-predator systems under the influence of global warming*, J. Appl. Math. Comput., **69** (2023), 4617–4643. 6
[36] S.-F. Tsao, H. Chen, T. Tisseverasinghe, Y. Yang, L. Li, Z. A. Butt, *What social media told us in the time of COVID-19: a scoping review*, The Lancet Digital Health, **3** (2021), e175–e194. 1
[37] World Health Organization, *Coronavirus disease (COVID-19) Virtual Press conference transcript*, 12 October, (2020). 1
[38] A. Yousef, A. A. Thirthar, A. L. Alaoui, P. Panja, T. Abdeljawad, *The hunting cooperation of a predator under two prey's competition and fear-effect in the prey-predator fractional-order model*, AIMS Math., **7** (2022), 5463–5479. 6